



This open access document is posted as a preprint in the Beilstein Archives at <https://doi.org/10.3762/bxiv.2022.11.v1> and is considered to be an early communication for feedback before peer review. Before citing this document, please check if a final, peer-reviewed version has been published.

This document is not formatted, has not undergone copyediting or typesetting, and may contain errors, unsubstantiated scientific claims or preliminary data.

**Preprint Title** Shift of reaction equilibrium at high pressure in the continuous synthesis of neuraminic acid

**Authors** Jannis A. Reich, Miriam Aßmann, Kristin Hölting, Paul Bubenheim, Jürgen Kuballa and Andreas Liese

**Publication Date** 02 März 2022

**Article Type** Full Research Paper

**ORCID® IDs** Jannis A. Reich - <https://orcid.org/0000-0002-6374-6630>; Miriam Aßmann - <https://orcid.org/0000-0002-1660-5253>

License and Terms: This document is copyright 2022 the Author(s); licensee Beilstein-Institut.

This is an open access work under the terms of the Creative Commons Attribution License (<https://creativecommons.org/licenses/by/4.0>). Please note that the reuse, redistribution and reproduction in particular requires that the author(s) and source are credited and that individual graphics may be subject to special legal provisions.

The license is subject to the Beilstein Archives terms and conditions: <https://www.beilstein-archives.org/xiv/terms>.

The definitive version of this work can be found at <https://doi.org/10.3762/bxiv.2022.11.v1>

# **Shift of reaction equilibrium at high pressure in the continuous synthesis of neuraminic acid**

Jannis A. Reich<sup>‡1</sup>, Miriam Aßmann<sup>‡2</sup>, Kristin Hölting<sup>2</sup>, Paul Bubenheim<sup>1</sup>, Jürgen Kuballa<sup>2</sup> and Andreas Liese<sup>\*1</sup>

Address: <sup>1</sup>Institute of Technical Biocatalysis, Hamburg University of Technology, Denickestr. 15, 21073 Hamburg, Germany and <sup>2</sup>GALAB Laboratories GmbH, Am Schleusengraben 7, 21029 Hamburg, Germany

Email: Prof. Andreas Liese – [liese@tuhh.de](mailto:liese@tuhh.de)

\* Corresponding author

‡ Equal contributors

## Abstract

The importance of a chemical that helps fight against Influenza is, in times of a global pandemic, self-evident. Many researchers see the continuous production in chemical industry as its next stepping stone. For these reasons, the synthesis of N-Acetylneuraminic acid in a continuous fixed-bed reactor by an immobilized epimerase and aldolase was investigated in detail. The immobilized enzymes showed high stability with half-life times > 173 days under storage condition (6 °C in buffer) and reusability over 50 recycling steps and was characterized regarding the reaction kinetics (initial rate) and scalability (different lab scales) in a batch reactor. In a continuous flow reactor reaction kinetics were studied. A high pressure circular reactor (up to 130 MPa) was applied for investigation of changes in the position of the reaction equilibrium. By this, equilibrium conversion, selectivity and yield were increased from 57.9% to 63.9%, 81.9% to 84.7% and 47.5% to 54.1%, respectively. This indicates a reduction in molar volume from GlcNAc and Pyr to Neu5Ac. The circular reactor in particular showed great potential to study reactions at high pressure while allowing for easy sampling. Additionally, an increase in affinity of pyruvate towards both tested enzymes was found with the application of pressure as measured in a decrease of  $K_I$  for the epimerase and  $K_M$  for the aldolase of 108 to 42 mM and 91 to 37 mM, respectively.

## Keywords

High Pressure; Neu5Ac; GlcNAc; ManNAc; Pyruvate; Immobilization; Enzyme; Epimerase; Aldolase; Continuous Fixed Bed Reactor

# Introduction

In times of a global pandemic, substances to boost the human immune system are self-explanatory. Sialic acids are such components that are produced and investigated for this reason as they can be found in cell membranes and play an important role in cell adhesion and signaling [1] and are for example investigated in Covid-19 research [2]. N-Acetyl-neuraminic acid (Neu5Ac) and the production thereof is described over the past three decades [3]. However until now no major breakthrough was achieved for its synthesis [4]. A review points out that: derivatives from Neu5Ac can inhibit viral enzymes [5]. Additionally some reports underline the importance of sialic acids (and not Neu5Ac in particular), of which Neu5Ac is the most prominent derivation [6]. Neu5Ac was approved as a food additive in the United States of America in 2016 and in the European Union and the Republic of China in 2017 [7]. Due to its importance, production of Neu5Ac is still being under investigation via enzymatic [4, 8] or whole cell production [9–11].

For this study, the enzymatic synthesis is under investigation for its simple reaction sequence (

Figure 1 and Figure 2) and high selectivity.



**Figure 1:** The first reaction step is the conversion from GlcNAc (left) to ManNAc (right).

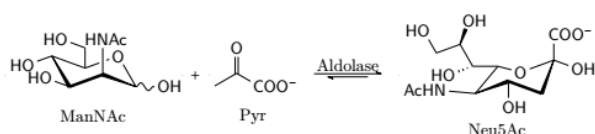


**Figure 2:** Second reaction step: Combination of ManNAc and Pyr to Neu5Ac.

Different research groups already made the effort to describe the reaction kinetics of the epimerase and aldolase at ambient pressure [4, 8]. In this study, the rate expressions from Groher et al. are being used [8]. So far, different approaches were taken to increase the position of the overall position of equilibrium using additional enzymes [12], temperature or high concentrations of the substrates [13].

In accordance with the principle of Le Chatelier, pressure can also be used to influence the position of equilibrium if the molar volume changes during the reaction [14]. High pressure processing is gaining traction for the enhancement of enzymes [15]. It has been shown that pressure can influence enzymatic reactions. Either in kinetics [16–18], enantiomeric excess [19] or stability [20] or the position of the equilibrium [17, 21]). State of the art for high pressure research is the use of pressurized batch reactors [22, 23].

Since continuous production and suitable reactors are getting more attention [24] and some believe that it will be the next milestone for industry [25, 26], the aim of this research was to first establish a continuous reactor at high pressure and then investigate the influence of pressure on the reaction sequence to produce Neu5Ac.

While there are high pressure processes established in food industry, that operate in a semi continuous manner, continuous reactors containing a High-performance liquid chromatography (HPLC) pump and a fixed bed reactor at high pressure are still a relatively new concept, already shown by Ötvös et al. up to 10 MPa (100 bar) [27] or reviewed by Plutschack et al. [28]. This work aims for pressures up to 130 MPa by the use of an Ultra High-performance liquid chromatography (UHPLC) pump.

# Results and Discussion

## Immobilization

For the biosynthesis of N-acetylneuraminic acid, two enzymes, the epimerase from *Pedobacter heparinus* and the aldolase from *Escherichia coli* K12 were produced in *E. coli* BL21(DE3). Both enzymes were purified and immobilized on different carriers to find for each enzyme the best choice for a stable and active enzyme preparation at the application under high pressure in continuous operation.

For screening purpose six different carriers were used to immobilize the epimerase and aldolase (Table 1). The carriers differ in their properties (size, hydrophobicity, binding type, and porosity). The quality of immobilization was evaluated regarding enzyme loading, activity, and reusability in repetitive batch experiments. Furthermore, the most suited carrier with immobilized enzyme was analyzed in long-term studies regarding the stability of the enzyme preparation.

**Table 1:** List of carriers for the screening used in this work (Lifetech Purolite)

Carrier	Functional group	Binding type	Hydrophobicity	Size [ $\mu\text{m}$ ]	Pores [ $\text{\AA}$ ]
Lifetech ECR8309F Amino methacrylate	amino	covalent	hydrophilic	150– 300	600– 1200
Lifetech ECR8204F Epoxy methacrylate	epoxy	covalent	hydrophilic	150– 300	300– 600
Lifetech ECR8285 Epoxy butyl methacrylate	epoxy	covalent	hydrophobic	250– 1000	450– 650
Lifetech ECR1030M Polymethacrylic DVB	none	adsorption	middle	300– 710	220– 340
Lifetech ECR8806F Octadecyl methacrylate	octadecyl	adsorption	hydrophobic	150– 300	400– 650
Lifetech ECR1090M Macroporous styrene	none	adsorption	hydrophobic	300– 710	200– 300

The enzymes were immobilized on six different carriers following the instruction of the supplier (Lifetech Purolite, Ratingen, Germany). The loading was quantified by

analysis of protein concentration before and after immobilization using the Bradford assay for protein quantification. Both enzymes were successfully immobilized on the carriers, see screening experiment (Figure 3). For the immobilized epimerase a maximal loading of 80 mg<sub>enzyme</sub>/g<sub>carrier</sub> was achieved. Two carriers reveal lower yields with enzyme loadings of 30 and 40 mg<sub>enzyme</sub>/g<sub>carrier</sub> (epoxy methacrylate, polymethacrylic DVB). The aldolase reveals the highest loadings with 80 mg<sub>enzyme</sub>/g<sub>carrier</sub> for the amino methacrylate and macroporous styrene carrier. The other analyzed loadings of the aldolase reveal a lower yield of 70 mg<sub>enzyme</sub>/g<sub>carrier</sub> (octadecyl methacrylate) and between 10–30 mg<sub>enzyme</sub>/g<sub>carrier</sub> for the other evaluated carrier.

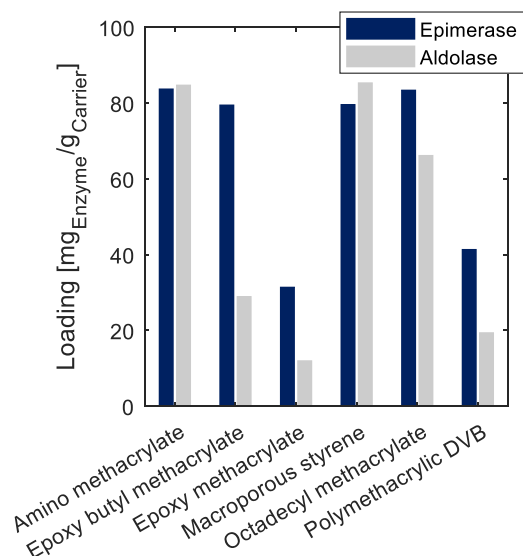


**Figure 3:** Enzyme loading after immobilization of the epimerase and aldolase on different carriers.

The activity of the immobilized enzymes was analyzed in small scale batch experiments in 1 mL reaction volume. The carrier was filtered, and a defined amount of each carrier was weighted out for the reaction. After addition of the substrate

samples were taken over the course of time and the specific activity was calculated (Figure 3 and Figure 4).

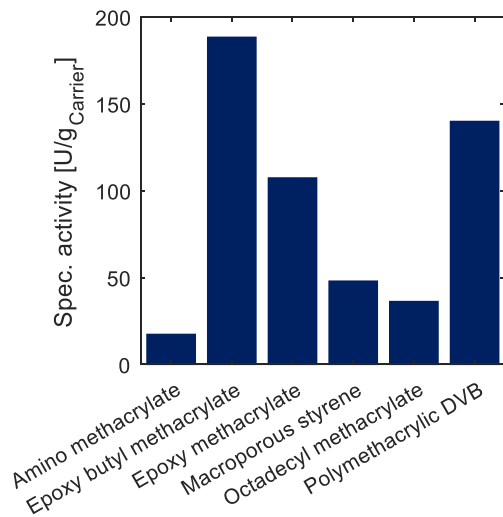


**Figure 4:** Evaluation of immobilized epimerase on different carriers regarding specific activities. Reaction conditions: 40 °C, pH 8, 100 mM Tris,  $U_{\text{shaking}} = 1400$  rpm,  $V = 1$  mL, 100 mM GlcNAc, 1 mM ATP, 1 mM  $MgCl_2$ , immo epimerase 1%(w/v).

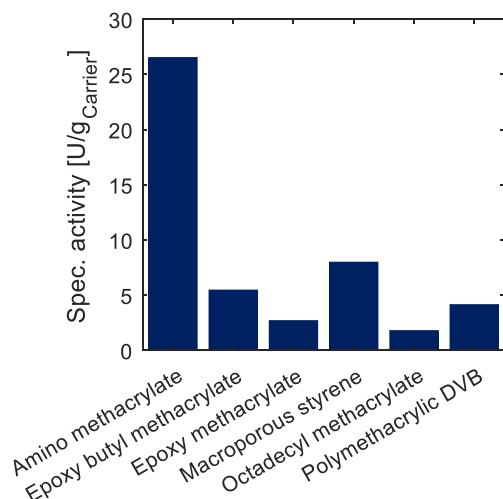


**Figure 5:** Evaluation of immobilized aldolase on different carriers in respect to specific activity. Reaction conditions: 40 °C, pH 8, 100 mM Tris,  $U_{\text{shaking}} = 1400$  rpm,  $V = 1$  mL, 100 mM N-acetyl-D-mannosamine, 250 mM pyruvate, immo aldolase 5%(w/v).

The product formation of the immobilized epimerase on amino methacrylate reveals the lowest calculated specific activity compared to other utilized carriers with less than 20 U/g<sub>carrier</sub>. The highest specific activity was achieved with two epoxy functionalized carrier (epoxy butyl methacrylate and polymethacrylic DVB) with over 100 U/g<sub>carrier</sub>. The Aldolase reveals immobilized on amino methacrylate the highest activities with about 25 U/g<sub>carrier</sub>. Compared to this, the result of all other specific activities was lower with less than 10 U/g<sub>carrier</sub>. Here the epoxy butyl methacrylate and macroporous styrene carrier reveal slightly more activity with over 5 U/g<sub>carrier</sub> compared to the others with less than 5 U/g<sub>carrier</sub>.

The selection of the most suitable carrier for the immobilization is important for the loading yield of the enzyme on the carrier and the yield of the activity. Both enzymes show on different material the best performance (epimerase: epoxy butyl methacrylate and aldolase: amino methacrylate). The microenvironment and material surrounding the enzyme have a significant influence on the enzyme activity [29].

A selection of the three most appropriate immobilized enzymes regarding the activity for the epimerase and aldolase for further investigations to analyze the reusability was done. The reusability was investigated via repetitive batch experiments in 1 mL small scale experiments with up to 5% (w/v) carrier which is in a range of industrial application of immobilized enzymes in a batch mode [30]. The immobilized epimerase shows in the application in repetitive batches the slightest activity loss using the epoxy methacrylate carrier (Figure 5). For the other analyzed activities on the different carriers the activity loss was much higher with 60% by using epoxy butyl methacrylate or 10% with polymethacrylate DVB.

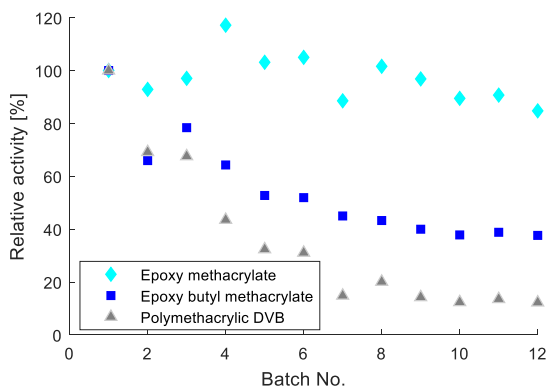


**Figure 6:** Relative activities in repetitive batch experiments of the immobilized epimerase on polymethacrylate DVB, epoxy methacrylate and epoxy butyl methacrylate. Reaction conditions: 40 °C, pH 8, 100 mM Tris,  $U_{\text{shaker}} = 1400$  rpm,  $V = 1$  mL, immo epimerase 1%(w/v), 100 mM N-acetyl-D-glucosamine, 1 mM ATP, 1 mM MgCl<sub>2</sub>

The reusability of the immobilized aldolase was analyzed with amino methacrylate, epoxy butyl methacrylate and macroporous styrene (Figure 7). All the carrier show high suitability in the repeated application with the highest loss of activity (35%) of the epoxy butyl methacrylate carrier and macroporous styrene carrier (25%).

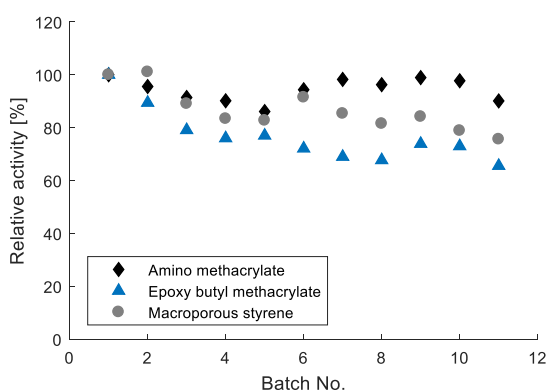


**Figure 7:** Relative activities in repetitive batch experiments of the immobilized aldolase on amino methacrylate, epoxy butyl methacrylate and macroporous styrene. Reaction condition: 40 °C, pH 8, 100 mM Tris,  $U_{\text{shaker}} = 1400$  rpm,  $V = 1$  mL, immo aldolase 5%(w/v), 100 mM N-acetyl-D-mannosamine, 250 mM pyruvate.

Both enzymes reveal a suitable reusability in the recycling study. Due to the measured activity, epoxy methacrylate was chosen as carrier for the epimerase and amino methacrylate for the aldolase, respectively. The immobilized enzymes were analyzed regarding their reusability over a higher number of 50 repetitive batches (Figure 8) and regarding their stability under storage and reaction condition (Table 1).

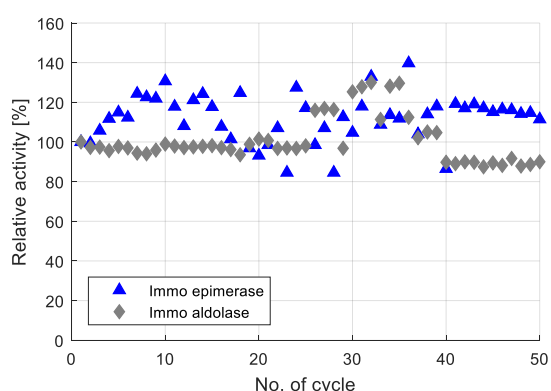


**Figure 8:** Recycling study of immobilized epimerase and aldolase. Assay conditions: 100 mM Tris, pH 8, 40 °C, shaking with 1000 rpm, V=1 mL. Between the batches the carrier was washed with 100 mM Tris pH 8 and stored until the next application at 4 °C. Reaction conditions: (i) immo epimerase: 100 mM N-acetyl-*D*-glucosamine, 1 mM ATP, 1 mM magnesium chloride, 10 g<sub>carrier</sub>/L, loading: 37.6 mg<sub>enzyme</sub>/g<sub>carrier</sub>; (ii) immo aldolase: 100 mM N-acetyl-*D*-mannosamine, 250 mM pyruvate, 70 g<sub>carrier</sub>/L, loading: 95.0 mg<sub>enzyme</sub>/g<sub>carrier</sub>.

**Table 2:** Storage, temperature and mechanic stability of immobilized epimerase and aldolase. \*No significant loss of activity in the analyzed time of the long-term study.

Condition of stability experiment	immo epimerase $\tau_{1/2}$ [d]	immo aldolase $\tau_{1/2}$ [d]
6 °C, w/o buffer	87	>179*

6 °C, with buffer	>173*	>179*
40 °C, with buffer	39	58
40 °C, with buffer and shaking	32	46

After 50 repetitive batches both enzymes reveal almost no loss of activity in the recycling study. The residual activity remains in a range around the starting activity indicating a high robustness of the selected preparations (Figure 8). The high fluctuation of the relative activity values can be explained by addition of several measurement errors. Besides the normal standard deviation, a number of more errors influencing the results, like the storage of the immobilized enzymes, irregularity of carrier washing after the application, the removal of the buffer before application as well as the sample taking and the sample preparation for the analytics. For further analysis, long-term studies were carried out to analyze the stability in respect to the influence of moisture on the storage condition, as well as temperature, and mechanical stress. The stability of the immobilized enzymes during the storage and the stability during the application of the enzyme is one important part for the economic use of the enzyme. Therefore, immobilized enzyme aliquots were stored under four different conditions: filtered and cooled at 6 °C, with buffer at 6 °C, with buffer at 40 °C and with buffer at 40 °C and shaking with 1000 rpm. During the storage time the activity was measured under standard activity conditions. By calculating of the residual activity, the stability was calculated by exponential fitting [31]. Because of inadequate correlation of the exponential fit for determination of deactivation a half-life time could not be calculated for all stability investigations. In these cases, the activity loss was minor and a fit by deactivation was not possible. During the experimental time the activity did not drop by 50%. For the immobilized enzymes, stored in buffer with cooling, in the

analyzed time of 179 days (immo aldolase) or 173 days (immo epimerase) no significant loss of activity was observed during the storage time (Table 2). For the immobilized aldolase no difference in stability during the storage of the filtered carrier with rest moisture or the wet stored carrier in buffer (>179 days) could be detected. For the immobilized epimerase, a high stability loss to a half-life of about 87 d without buffer compared to the wet stored carrier with >173 d was detected. The strongest influence is evoked through heating of the immobilized enzymes by decreasing the half-life time to 39 d or 58 d for the immobilized epimerase or aldolase under continuous exposure of the temperature, respectively. The mechanical stress through mixing of the immobilized enzyme decreases the stability by about 20% compared to the comparative study without shaking. Concluding to the stability investigations, it can be concluded that both selected enzyme preparations reveal appropriate stability for the continuous application under high pressure.

## Fixed Bed and Circulation Reactor

In order to investigate the effect of pressure on the chosen reaction, a continuously operated fixed bed reactor of immobilized enzyme, was used (Figure 9). By setting a high flow rate, determination of the reaction rate via initial rate measurement is possible. The pressure was built up using capillaries with a small inner diameter (25  $\mu\text{m}$  and 50  $\mu\text{m}$ ) (law of Hagen-Poiseuille [32]).

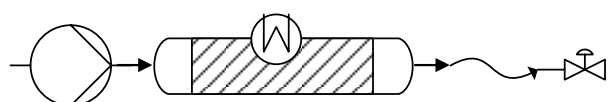


**Figure 9:** Reactor set-up (left to right): UHPLC pump, heated fixed bed reactor, capillaries (ID: 25  $\mu\text{m}$  or 50  $\mu\text{m}$ , length: 30 cm), back pressure regulator (up to 30 MPa).

The fixed bed reactor was utilized to investigate the reaction kinetics. Residence time distribution (RDT) of the fixed bed reactor was calculated (Eq. (1)) and used to, calculate the mean residence time (Eq. (2)).

$$E(t) = \frac{S(t)}{\int S(t)dt} \quad (1)$$

$$\bar{t} = \int t \cdot E(t)dt \quad (2)$$

The RDT was measured by inserting the reactor into an HPLC, replacing the regular separation column. Hereby the mean residence time of the reactor was calculated to be 66% of the quotient of reactor volume and flow rate.

If the position of the equilibrium is to be investigated, high residence times and small flow rates need to be applied. Since the pressure drop over a capillary depends on the flow rate, pressure could not sufficiently being build up when investigating the equilibrium. For this reason, the fixed bed reactor was changed into a circular reactor (Figure 10). In this set-up the flow rate can be set (almost) freely to achieve the desired pressure (mixing time is affected when the flow rate is low).

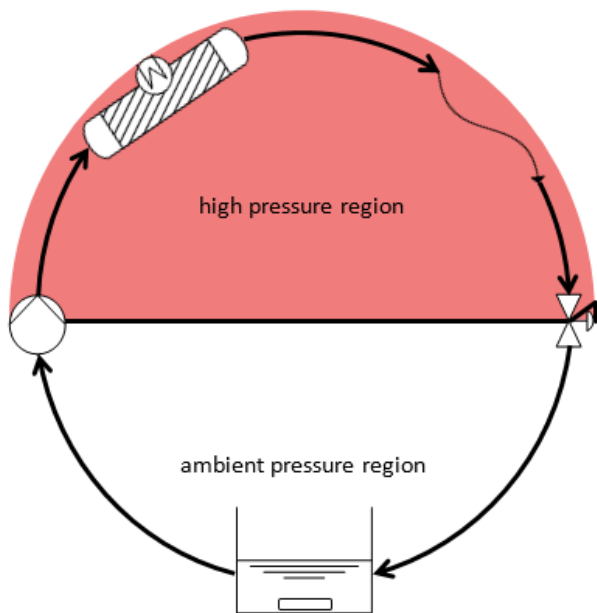


**Figure 10:** Circular reactor, vessel mixing was achieved with a magnetic stirrer and samples were taken directly from the vessel.

### Kinetics

As a proof of principle, reaction kinetics were measured for the immobilized epimerase. With no inhibitors or backward reactions present, the reaction rate can be expressed as a Michaelis-Menten rate expression (Eq. (3)) which was used for the fit in Figure 11. The resulting kinetic parameters are shown with 95% confidence intervals in Table 3. All particles were pestled to remove potential diffusion limitation. All experiments were conducted at 40 °C and in potassium phosphate buffer.

$$v = \frac{v_{max} c_{GlcNac}}{K_M + c_{GlcNac}} \quad (3)$$

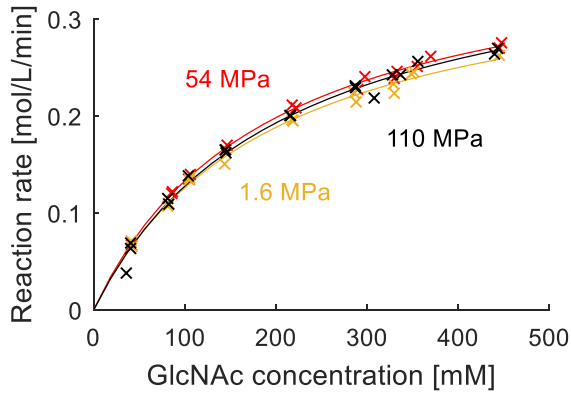


**Figure 11:** Measured reaction rate for the epimerase. The dashed line is the fit according to Eq. (3) Conditions: 40 °C, flow rates: 1.6 MPa at 2 mL/min, 54 MPa and 110 MPa at 1.8 mL/min, reactor volume: 0.21 mL, 10 mM potassium phosphate buffer 7.50, 1 mM ATP, 1 mM MgCl<sub>2</sub>, 55 mg epimerase.

**Table 3:** Kinetic parameters. The error given for pressure is the median average difference. The error given for the kinetic parameters indicates the confidence interval (95%) in the regression.

Pressure [MPa]	$K_M$ [mM]	$a_{sp}$ [ $\mu\text{mol/g}_{\text{carrier}}/\text{min}$ ]	$v_{max}$ [mol/L/min]
$1.6 \pm 0.1$	$195 \pm 26$	$1324 \pm 77$	$0.37 \pm 0.02$
$54 \pm 3.8$	$208 \pm 34$	$1400 \pm 104$	$0.41 \pm 0.03$
$110 \pm 9.3$	$193 \pm 93$	$1388 \pm 47$	$0.39 \pm 0.01$

The influence of pressure on the inhibition by pyruvate was measured and is shown in Figure 12. The following equation was used for non-linear regression:

$$v = \frac{a}{K_M \cdot \left(1 + \frac{c_{Pyr}}{K_I}\right) + c_{GlcNAc}} \quad (4)$$

With  $a$  as a factor for fitting to account for decrease in total activity due to time,  $K_M$  as the determined Michaelis-Menten constant,  $c_{Pyr}$  and  $c_{GlcNAc}$  as concentration of pyruvate and GlcNAc, respectively and  $K_I$  as inhibition constant.

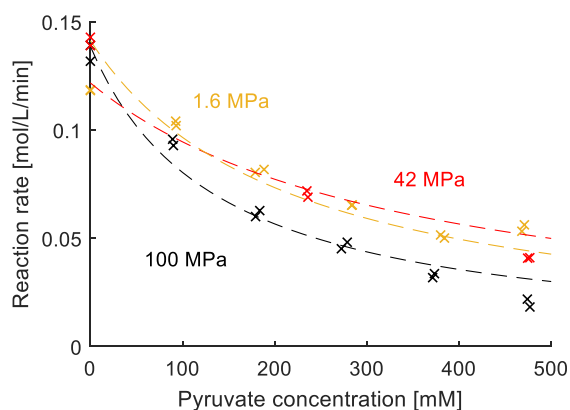


**Figure 12:** Measured reaction rate as a function of pyruvate and pressure. Dashed lines are fitted according to Eq. (4). 40 °C, volume flow: 2 mL/min, 440 mM GlcNAc, 100 mM buffer, 0.21 mL reactor volume, 2.25 min waited for steady state.

**Table 4:** Determined inhibition constant for pyruvate for the epimerase reaction. The error given for the kinetic parameters indicates the confidence interval (95%) in the regression.

Pressure [MPa]	$K_I$ [mM]
1.6	$108 \pm 021$
42	$67 \pm 011$
100	$43 \pm 010$

The value for the inhibition constant is in the same order of magnitude as results show from other groups, measured at ambient pressure ( $0.146 \pm 0.019$  mol/L [4]). Since the  $K_I$  value changes with pressure (Table 4), the concentrations were kept constant once

more and only the pressure was varied, resulting in Figure 13 (left). By rearranging Eq. (4) and inserting the kinetic parameters previously calculated, the inhibition constant was calculated (Figure 13 (right)).

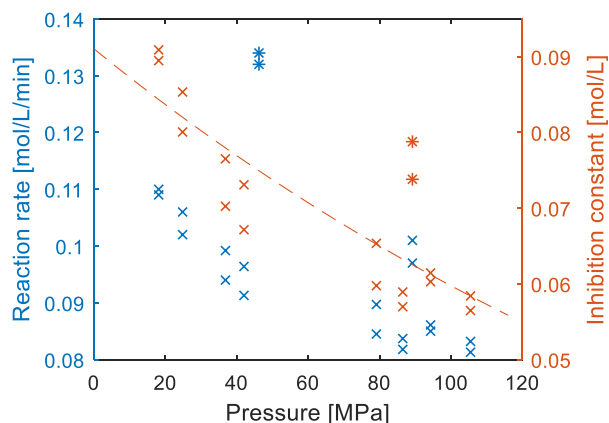


**Figure 13:** Measured reaction rate (left) and determined inhibition constant by pyruvate (right) at different pressure. 450 mM GlcNAc, 400 mM pyruvate, 2 mL/min, 40 °C, 0.21 mL reactor volume. Points determined as outliers are marked using asterisks.

The change in molar volume introduced by the coupling of pyruvate to the enzyme was calculated by using the exponential fit (Figure 13). It was calculated to be  $-12.9 \pm 5.5$  mL/mol (the values at 50 MPa and 89 Mpa were considered to be outliers and not included in the calculation).

Kinetic studies of the aldolase do show an increase in affinity of pyruvate towards the enzyme (Figure 14). The  $K_M$  values were calculated to be  $91 \pm 45$  mM and  $37 \pm 10$  mM for 2 MPa and 115 MPa, respectively. From the change in the Michaelis-Menten constant, a change in volume for the binding of pyruvate to the enzyme was calculated to be -20 mL/mol. Calculated kinetic parameters are given in Table 5. Since

Neu5Ac is acidic, 200 mM of buffer solution was used with addition of  $K_2HPO_4$  to neutralize the solution to pH 7.2. Using the Haldane relation, the equilibrium constant was calculated to be 27 L/mol and 48 L/mol for 2 MPa and 115 MPa, respectively.

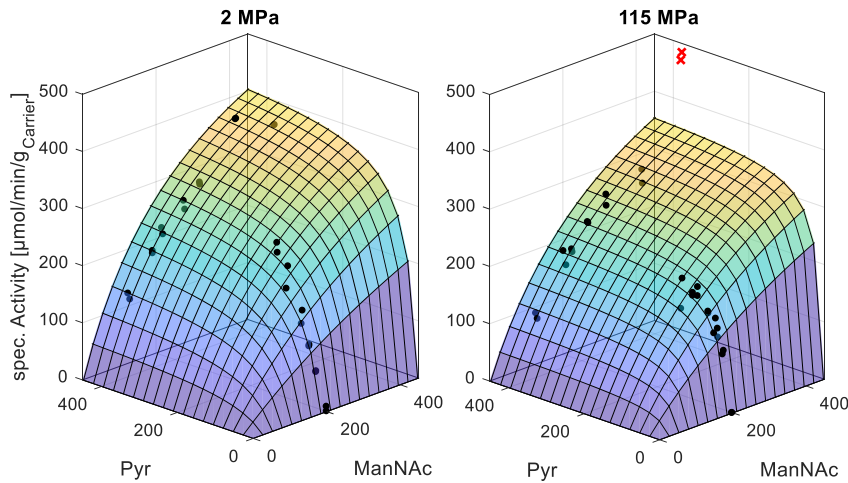


**Figure 14:** Measured kinetic of the aldolase when varying the pyruvate and ManNAc concentration (given in mM) at different pressure. Reaction conditions: 40 °C, flow rate: 1.5 - 2 mL/min, reactor volume: 0.70 mL, 100 mM potassium phosphate buffer pH 7.50, 179.80 mg aldolase. Immobilizate was pestled.

**Table 5:** Calculated kinetic parameters at ambient and high pressure. Rate expression adopted from Groher et al. [8].

<b>Forward reactions</b>	2 MPa	115 MPa
$a_{sp,max}$ [U/g <sub>carrier</sub> ]	$650 \pm 150$	$630 \pm 130$
$K_{M,ManNAc}$ [mM]	$230 \pm 110$	$320 \pm 120$
$K_{M,Pyr}$ [mM]	$91 \pm 45$	$37 \pm 10$

<b>Backward reactions</b>	2.5 MPa	93 MPa
$K_{M,Neu}$ [mM]	$650 \pm 300$	$365 \pm 260$
$a_{sp,max}$ [U/g <sub>carrier</sub> ]	$743 \pm 230$	$403 \pm 170$

### Position of Equilibrium

The position of the equilibrium was determined by using the circular reactor. The ratio of product and substrates was calculated for each sample and converges to the equilibrium constant at the given conditions.

The equilibrium constant for the first reaction (one-to-one) was insensitive to pressure. For the second reaction (aldolase), the calculated equilibrium constant is shown in Figure 15. Since this reaction step is a two-to-one-reaction, a reduction of molar volume was expected which led to a positive influence of pressure (principle of Le' Chatelier). The change in volume was calculated to be  $(-16.0 \pm 1.2)$  mL/mol.

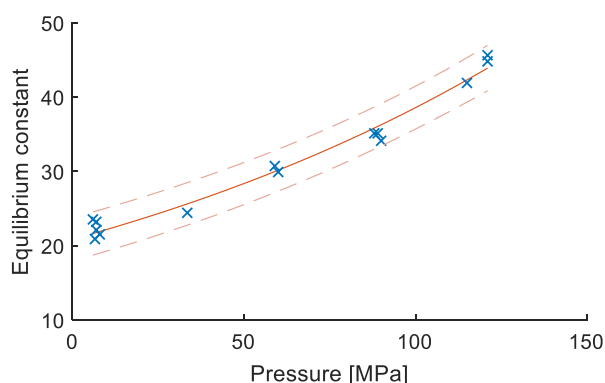


**Figure 15:** Aldolase: Change of equilibrium constant at different pressures. Starting concentration were varied. 100 mM with 250 mM and 100 mM with 100 mM of ManNAc and pyruvate, respectively, 41 °C, reaction time at least 12 h, total working volume 4 mL, flow rate 1.5 mL/min, 272.3 mg aldolase. Used regression is an exponential fit according to Eq.(7).

Both immobilizates were added into one reactor and GlcNAc and Pyr were added as substrates to produce Neu5Ac. The resulting progress curve is shown in Figure 16. In order to measure changes in concentration with a high resolution, a high working volume was chosen and the enzyme concentrations were reduced, leading to slower conversion. The pressure was then varied which led to a change in substrate and product concentration, indicating that the system was sensitive to pressure.

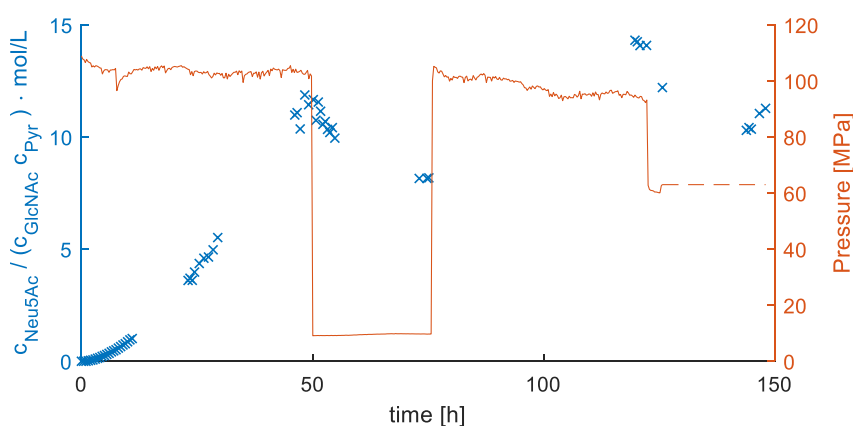


**Figure 16:** Progress curve of the circular reactor with both reactions and at varying pressure. Starting conditions: 300 mM ManNAc and 300 mM Pyr, 100 mM potassium phosphate buffer at a pH of 7.50, 2 mL/min, total working volume: about 15 mL, 40 °C, 0.35 mL reactor volume, 1:10 (v/v) epimerase: aldolase, total mass: 85.4 mg.

Figure 16 shows the two advantages of the high pressure circulation reactor over a pressurized batch reactor: Firstly: Without the use of special pressure valves, samples can be taken. Secondly: Pressure can be changed while the reaction is ongoing. If pressure is only changed up to 30 MPa the operation can continue. If larger changes in pressure are needed, the pump can be shut down, capillaries quickly be added or removed and the pump turned on again for a minimal downtime.

The combined reaction was, like the aldolase reaction, positively influenced by pressure. This was shown with the ratio of product and substrates (with the equilibrium constant  $K$  as the asymptote) as well as conversion, selectivity and yield. While conversion, selectivity and yield depend on the ratio of substrate, the equilibrium constant can be used for other ratios as well.

**Table 6:** Changes in conversion, selectivity and yield at different pressures. Same reaction conditions as Figure 16.

Pressure [MPa]	Conversion [%]	Selectivity [%]	Yield [%]
9.6	57.9	81.9	47.4
60.8	60.4	82.7	50.0
95.0	63.9	84.7	54.1

## Conclusion

An epimerase and an aldolase were investigated in order to continuously produce N-Acetylneuraminic acid under increased pressure. Both enzymes were successfully immobilized with high stability and used to catalyze a reaction starting from N-acetyl-D-glucosamine and pyruvate. In addition, pressure up to 130 MPa was successfully used to increase the conversion by 10%, the selectivity by 3% and the yield by 14% (to 63.9%, 84.7% and 54.1%, respectively). The equilibrium constant was approximated using concentrations and increased with pressure indicating a reduction in molar volume. The circular reactor setup allowed easy sampling and enabled the analysis of the resulting progress curve. The results for the epimerase indicate that

some inconspicuous reactions, such as the inhibition by pyruvate, can be influenced by pressure.

Pyruvate in particular shows an increased affinity towards both investigated enzymes. Given the importance of pyruvate [33–35], an approach of testing different pyruvate converting enzymes, if this trend holds true, might be of interest.

## **Experimental**

### **Methodology**

#### **Genes and expression strains**

The gene of the epimerase (N-acyl-D-Glucosamine 2-epimerase, EC 5.1.3.8) from *Pedobacter heparinus* was ordered as codon optimized gBlocks gene fragment (Integrated DNA Technologies, Leuven, Belgium). The gene for the aldolase (N-acetylneuraminate lyase, EC 4.1.3.3) was amplified from the genomic DNA of *Escherichia coli* K12. The genes of the enzymes were cloned into the expression vector pETDuet-1™ (Novagen®, Merck KGaA, Darmstadt, Germany). For expression *E. coli* BL21 (DE3) strains were used.

#### **Activity assays**

To compare the activities of both enzymes a standard activity assay was used for the free and immobilized enzymes. For the epimerase the reaction conditions were 100 mM Tris, pH 8, 40 °C, 100 mM N-acetyl-D-glucosamine, 1 mM adenosine triphosphate, 1 mM magnesium chloride and 10 g/L immobilized enzyme or 2.5 mg/L free enzyme. For the aldolase the reaction conditions were 100 mM Tris, pH 8, 40 °C, 100 mM N-acetyl-D-mannosamine, 250 mM pyruvate and 50 g/L immobilized enzyme or 100 mg/L free enzyme.

#### **Repetitive batch study**

The reusability was analyzed with 10 mg immobilized epimerase (in triplicate) or 70 mg of immobilized aldolase (in duplicate) in 2 mL micro reaction tubes. The reaction was started by addition of 1 mL substrate solution and the reaction was run for 30 min and analyzed by product formation. Afterwards the remaining substrate was removed and the carriers were washed twice with 100 mM Tris, pH 8 and used for the next cycle or stored at 6 °C for the next experiment. For each enzyme 50 repetitive batches was analyzed.

### **Stability study**

For stability investigations, the immobilized enzyme was aliquoted into 2 mL micro reaction tubes (10 mg immobilized epimerase or 50 mg immobilized aldolase) and stored under four different conditions: 6 °C with residual moisture, in 20 mM sodium phosphate buffer pH 7.5 with 6 °C, 40 °C and 40 °C with shaking at 1000 rpm. The residual moisture means the immobilized enzyme after filtration under vacuum. The aliquots were stored, and activity was measured in regularly time points over the time of storage. For each measuring point the initial activity was analyzed with a standard activity assay.

### **High performance liquid chromatography (HPLC)**

For quantification of the product N-acetylneuraminic acid an Agilent HPLC system connected with a variable wavelength detector at 210 nm was used. Separation was realized with a Nucleogel Sugar 810H column (Macherey Nagel, Düren, Germany). Injection was set to 10 µL and compounds were eluted by an isocratic flow of 0.1% phosphoric acid with 30 °C. The retention order was N-acetylneuraminic acid (8.1 min), pyruvate (9.5 min) and N acetylglucosamine (11.1 min).

### **Enzymatic quantification of N-acetyl-D-mannosamine**

The quantification of ManNAc for the epimerase activity was realized with an enzymatic quantification assay as described in Klermund et al using N-acylmannosamine 1-

dehydrogenase (ManDH, EC. 1.1.1.233) [36]. The assay was performed in 100 mM Tris-HCl pH 8 with up to 0.2 mM ManNAc, 2 mM NAD and 0.05 mL ManDH solution with 3 kU/mL. After starting the reaction, the assay was incubated for 30 min at room temperature. The resulting NADH concentration was measured with an Eppendorf spectrophotometer at 340 nm.

### **High-Pressure set-up**

An HPLC-pump by Shimadzu Deutschland (Duisburg, Germany) was applied in order to generate a steady flow. For the reactor, an empty HPLC column by ISERA GmbH (Düren, Germany) was used.

Pressure was built up using capillaries with a small inner diameter (50 µm).

If the position of the equilibrium was investigated, high residence times were needed resulting in low flow rates and pressure built up.

In order to handle this bottle neck, a circular reactor was designed. A flow rate can be chosen in order to achieve the desired pressure (most of the time 1.7 – 2 mL/min).

Another advantage is the reduction of film diffusion on the carriers.

A key advantage of this setup is that sampling and reaction at high pressure occur simultaneously and progress curves can be measured in one reactor. Prior publications investigating high pressure batch reactors needed to conduct several experiments and open the reactors at different points in time [37, 22]. Not only that, the circular reactor also allows for a change in pressure via the back pressure regulator.

A magnetic stirrer was used to mix the fluid in a vessel from which the pump draws its feed.

**Chemicals** were ordered by Biosynth Carbosynth (United Kingdom) and used with no further purification.

Buffers: potassium phosphate buffer: 5.3 mL of 0.2 M potassium phosphate (mono) ( $\text{KH}_2\text{PO}_4$ ) with 94.7 mL of 0.2 M potassium phosphate (di) ( $\text{K}_2\text{HPO}_4$ ) in 100 mL resulting in 200 mL of 100 mM – the buffer was measured and corrected to pH 8.00 afterwards by adding more mono- or di-potassium.

1 M Tris: 121.14 g tris(hydroxymethyl)aminomethane in 800 mL  $\text{H}_2\text{O}$  with HCl. Followed with adjusting to 1 L using  $\text{H}_2\text{O}$ .

### **Analytcs**

Analysis was conducted according to Zimmerman and Kragl using Eurocat H type (KNAUER Wissenschaftliche Geräte GmbH (Berlin, Germany)) in an HPLC system (0.8 mL/min, 65 °C, 55 °C for RI, 5mM  $\text{H}_2\text{SO}_4$ ).

The retention order was N-acetylneuraminic acid (14 min), pyruvate (15.5 min), N-Acetyl-D-Mannosamine (19 min) and N acetylglucosamine (20 min).

**The packing of the enzymatic bed** was done via sedimentation of the particles. For this a slurry of particles was produced in buffer solution (10 or 100 mM  $\text{KPi}$  buffer at pH 7.5) and taken up using a syringe. In parallel, the reactor was filled with buffer solution from the bottom up. The syringe was then placed at the top of the reactor forming a water bridge allowing the particles to sediment. Once the reactor was filled, it was shaken in order for the bed to settle and refilled if needed.

After the bed was packed, buffer was pumped through it in order to compress it. The reactor was then opened and new particles were introduced so that the whole space was occupied.

### **Residence time distribution**

In order to check whether or not this method yields similar packed beds, the residence time distribution (RTD) was measured and compared. The pump, autosampler and refraction index (RI) detector were used to measure the RDT (HPLC 1100er Series by Agilent). Injected were 5  $\mu$ L of 10 mM buffer as a tracer with an injection speed of 1 mL/min resulting in a rapid injection. Volume flow was set to 0.1, 0.35 and 0.5 mL/min. The used reactor was an empty UHPLC column by ISERA (length 50 mm ID 3 mm). The RI was measuring the refraction about twice a second.

A tracer peak was injected via the autosampler and measured using a RI detector (KNAUER Wissenschaftliche Geräte GmbH, Berlin, Germany).

When setting the flow rate to 0.35 mL/min, a mean residence time of  $1.5 \pm 0.01$  min was calculated. The mean residence time of the system itself needs to be taken into account. It was determined to be  $0.801 \pm 0.003$  min.

The residence time distribution of the reactor was calculated using the assumption that the cumulative distributions are additive with respect to time. As a test, the obtained distribution of the reactor was convoluted with the distribution of the system and a result similar to the measured distribution of both was obtained (Figure 17).

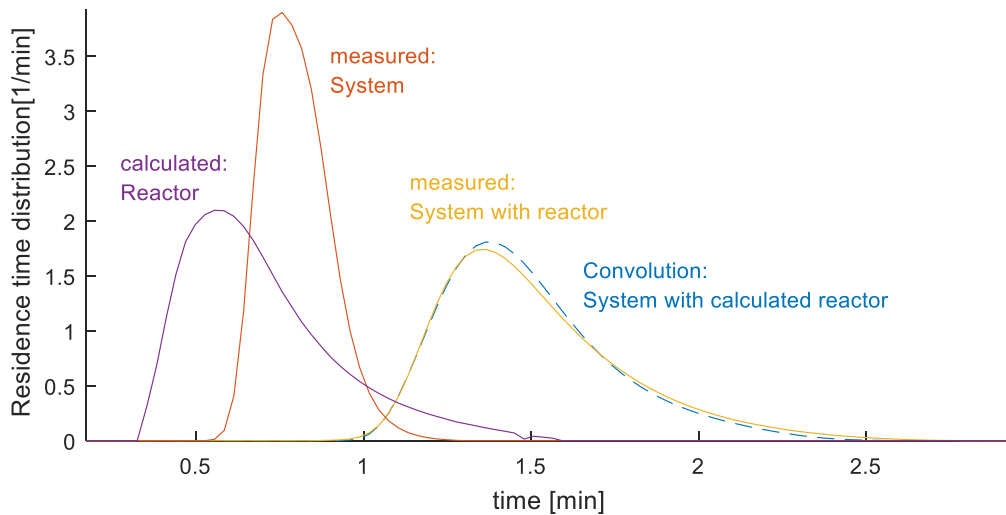


**Figure 17:** Residence time distributions of the stand-alone system, and reactor integrated into the system. Flow rate: 0.35 mL/min, reactor volume: 0.35 mL, filled with 74 to 80 mg of particles, 5  $\mu$ L of 10 mM potassium phosphate buffer were used as tracer and injected with a speed of 1 mL/min

The mean residence time is 0.7 min (in contrast to 1 min which is obtained by dividing the whole reactor volume by flow rate) using particles with the original size distribution. Since the diameter of the original particles is 0.5 mm and the inner diameter of the reactor only 3 mm, wall effects occur [38, 39].

When using pestled particles, the mean residence time was 0.66 min when pumping 0.21 mL/min through a reactor volume of 0.21 mL. When using pestled particles the residence time distribution is assumed to be narrow because the RTD of the system and of the whole setup are similar in shape and just shifted in time.

Integration was conducted using Matlab 2017a and 2018a using the trapz function.

The given values for  $\tau$  do not account for the porosity of the packed bed. They will be calculated via

$$\tau = \frac{V}{\dot{V}} \quad (5)$$

With  $V$  as the volume of the empty reactor (in mL) and  $\dot{V}$  as the volumetric flow rate (in mL/min).

## Kinetics

When kinetic parameters were calculated via regression, the error given represents the 95% confidence intervals.

Since the pump is intended for UHPLC application, a mixing chamber for up to four eluents is installed. In this study, the mixing chamber was used to change the concentration of the substrate to measure the reaction rate. The homogeneity of the fluid produced with the mixing chamber was ensured via a UV detector (Sup. Tab X). The order of the concentrations was randomized so that concentrations would not systematically carry over to the next experiment.

Reaction rate was calculated using the product concentration ( $c_{MannAc}$ ), hydraulic residence time ( $\tau$ ) and volume fraction ( $f_V$ )

$$v = \frac{c_{MannAc}}{f_V \cdot \tau} \quad (6)$$

The volume fraction was determined to be 0.66 for pestled particles.

## Equilibrium

The change in volume introduced by reactions (such as the binding of pyruvate to the enzyme) was calculated via the kinetic constant  $K_M$  and  $K_I$ . Since those approximate an equilibrium constant, the following equation was used:

$$K(p) = K(0 \text{ MPa}) \cdot \exp\left\{-\frac{\Delta V}{RT} \cdot p\right\} \quad (7)$$

Conversion is calculated via a closed mass balance with  $c_{GlcNAc}(0) = c_{GlcNAc}(t) + c_{ManNAc}(t)$ :

$$X(t) = \frac{c_{ManNAc}(t)}{c_{GlcNAc}(t) + c_{ManNAc}(t)} \quad (8)$$

For a reaction with different products or a sequence of reactions, selectivity is calculated using the product concentration:

$$S(t) = \frac{c_{Neu5Ac}(t)}{c_{ManNAc}(t) + c_{Neu5Ac}(t)} \quad (9)$$

## Acknowledgements

Intellectual support from the research alliance protP.S.I. is thankfully acknowledged. Jannis A. Reich would also like to thank Frederic Perz and Fernando Lopez-Haro for discussions and input.

## Funding

Financial funding was provided by the Federal Ministry of Education and Research (number: 031B0405A) and is greatly appreciated.

## References

1. Varki, A. *Trends Mol. Med.* **2008**, *14* (8), 351–360.  
doi:10.1016/j.molmed.2008.06.002
2. Altalhi, T. A.; Alswat, K.; Alsanie, W. F.; Ibrahim, M. M.; Aldalbahi, A.; El-Sheshtawy, H. S. *J. Mol. Struct.* **2021**, *1228*, 129459.  
doi:10.1016/j.molstruc.2020.129459
3. Kragl, U. *Reaktionstechnik biokatalytischer Prozesse am Beispiel der kontinuierlichen enzymatischen Synthese von N-Acetylneuraminsäure*; Forschungszentrum, Zentralbibliothek: Jülich, 1992.
4. Zimmermann, V.; Hennemann, H.-G.; Dausmann, T.; Kragl, U. *Applied microbiology and biotechnology* **2007**, *76* (3), 597–605. doi:10.1007/s00253-007-1033-6
5. Maru, I.; Ohnishi, J.; Ohta, Y.; Tsukada, Y. *J. Biosci. Bioeng.* **2002**, *93* (3), 258–265. doi:10.1016/S1389-1723(02)80026-3
6. Lakdawala, S. S.; Jayaraman, A.; Halpin, R. A.; Lamirande, E. W.; Shih, A. R.; Stockwell, T. B.; Lin, X.; Simenauer, A.; Hanson, C. T.; Vogel, L.; Paskel, M.; Minai, M.; Moore, I.; Orandle, M.; Das, S. R.; Wentworth, D. E.; Sasisekharan, R.; Subbarao, K. *Nature* **2015**, *526* (7571), 122–125. doi:10.1038/nature15379

7. Zhu, W.; Chen, X.; Yuan, L.; Wu, J.; Yao, J. *Molecules* **2020**, *25* (21).  
doi:10.3390/molecules25215141
8. Groher, A.; Hoelsch, K. *J. Mol. Catal. B: Enzym.* **2012**, *83*, 1–7.  
doi:10.1016/j.molcatb.2012.05.016
9. Lin, B.-X.; Zhang, Z.-J.; Liu, W.-F.; Dong, Z.-Y.; Tao, Y. *Applied microbiology and biotechnology* **2013**, *97* (11), 4775–4784. doi:10.1007/s00253-013-4754-8
10. FERMENTATIVE PRODUCTION OF N-ACETYLNEURAMINIC ACID - European Patent Office - EP 3473644 A1. 17196925.6, Oct 17, 2017.
11. Zhu, D.; Zhan, X.; Wu, J.; Gao, M.; Zhao, Z. *Biotechnology letters* **2017**, *39* (1), 55–63. doi:10.1007/s10529-016-2215-z
12. Abu, R.; Woodley, J. M. *ChemCatChem* **2015**, *7* (19), 3094–3105.  
doi:10.1002/cctc.201500603
13. Hussain, M. I.; Zhang, X.; Lv, X.; Basharat, S.; Shahbaz, U.; Li, J.; Du, G.; Liu, L.; Liu, Y. *Syst Microbiol and Biomanuf* **2022**, *2* (1), 130–146. doi:10.1007/s43393-021-00050-y
14. Atkins, P. W.; Paula, J. de. *Physikalische Chemie*, 8., [komplett überarb.] Aufl.; Wiley-VCH Verl.: Weinheim, 2006.
15. Eisenmenger, M. J.; Reyes-De-Corcuera, J. I. *Enzyme Microb. Technol.* **2009**, *45* (5), 331–347. doi:10.1016/j.enzmictec.2009.08.001

16. Kitahara, R.; Oyama, K.; Kawamura, T.; Mitsuhashi, K.; Kitazawa, S.; Yasunaga, K.; Sagara, N.; Fujimoto, M.; Terauchi, K. *Sci. Rep.* **2019**, *9* (1), 12395.  
doi:10.1038/s41598-019-48693-1
17. Luong, T. Q.; Erwin, N.; Neumann, M.; Schmidt, A.; Loos, C.; Schmidt, V.; Fändrich, M.; Winter, R. *Angew. Chem. Int. Ed. Engl.* **2016**, *55* (40), 12412–12416. doi:10.1002/anie.201605715
18. Eyring, H.; Magee, J. L. *J. Cell. Comp. Physiol.* **1942**, *20* (2), 169–177.  
doi:10.1002/jcp.1030200205
19. Berheide, M.; Peper, S.; Kara, S.; Long, W. S.; Schenkel, S.; Pohl, M.; Niemeyer, B.; Liese, A. *Biotechnology and bioengineering* **2010**, *106* (1), 18–26.  
doi:10.1002/bit.22650
20. Kaushik, N.; Rao, P. S.; Mishra, H. N. *Food research international (Ottawa, Ont.)* **2017**, *100* (Pt 1), 885–893. doi:10.1016/j.foodres.2017.07.056
21. Lomelí-Martín, A.; Martínez, L. M.; Welti-Chanes, J.; Escobedo-Avellaneda, Z. *Foods (Basel, Switzerland)* **2021**, *10* (4). doi:10.3390/foods10040878
22. Hackbusch, S.; Noirungsee, N.; Viamonte, J.; Sun, X.; Bubenheim, P.; Kostka, J. E.; Müller, R.; Liese, A. *Mar. Pollut. Bull.* **2020**, *150*, 110683.  
doi:10.1016/j.marpolbul.2019.110683
23. Shkolnikov, H.; Belochvostov, V.; Okun, Z.; Shpigelman, A. *Innov. Food Sci. Emerg. Technol.* **2020**, *59*, 102273. doi:10.1016/j.ifset.2019.102273

24. Gambacorta, G.; Sharley, J. S.; Baxendale, I. R. *Beilstein J. Org. Chem.* **2021**, *17*, 1181–1312. doi:10.3762/bjoc.17.90
25. Elliott, M.; Makatsoris, H. *Chimica Oggi - Chemistry Today* **2020**, *38* (3), 8-9.
26. Vilé, G.; Amann, F.; Bourne, S.; Elliott, M.; Wiles, C.; Houldsworth, S.; Vizza, A.; Gemoets, H.; Ramakrishnan, S.; Bandichhor, R.; Kaaden, A.; Heck, J.; Noel, T.; Nonnenmacher, M.; Loureiro, R.; Kirschneck, D.; Ni, X.-W.; Lovett, D.; Khinast, J.; Dubay, Bill, Dapremont, Oliver; Muldowney, M. *Chimica Oggi - Chemistry Today* **2020**, *38* (3), 14-30.
27. Ötvös, S. B.; Georgiádes, A.; Mándity, I. M.; Kiss, L.; Fülöp, F. *Beilstein J. Org. Chem.* **2013**, *9*, 1508–1516. doi:10.3762/bjoc.9.172
28. Plutschack, M. B.; Pieber, B.; Gilmore, K.; Seeberger, P. H. *Chem. Rev.* **2017**, *117* (18), 11796–11893. doi:10.1021/acs.chemrev.7b00183
29. Bolivar, J. M.; Nidetzky, B. *Molecules* **2019**, *24* (19).  
doi:10.3390/molecules24193460
30. Basso, A.; Serban, S. *Molecular Catalysis* **2019**, *479*, 110607.  
doi:10.1016/j.mcat.2019.110607
31. Liese, A.; Hilterhaus, L. *Chem. Soc. Rev.* **2013**, *42* (15), 6236–6249.  
doi:10.1039/c3cs35511j

32. Suter, S. P.; Skalak, R. *Annu. Rev. Fluid Mech.* **1993**, *25* (1), 1–20.  
doi:10.1146/annurev.fl.25.010193.000245
33. Tonin, F.; Arends, I. W. C. E. *Beilstein J. Org. Chem.* **2018**, *14*, 470–483.  
doi:10.3762/bjoc.14.33
34. Menefee, A. L.; Zeczycki, T. N. *FEBS J.* **2014**, *281* (5), 1333–1354.  
doi:10.1111/febs.12713
35. Baik, S. H.; Kang, C.; Jeon, C., II; Yun, S. E. *Biotechnol. Tech.* **1999**, *13* (1), 1–5.  
doi:10.1023/A:1008865212773
36. Klermund, L.; Riederer, A.; Hunger, A.; Castiglione, K. *Enzyme Microb. Technol.* **2016**, *87-88*, 70–78. doi:10.1016/j.enzmictec.2016.04.006
37. Schedler, M.; Hiessl, R.; Valladares Juárez, A. G.; Gust, G.; Müller, R. *AMB Express* **2014**, *4*, 77. doi:10.1186/s13568-014-0077-0
38. Dixon, A. G.; Nijemeisland, M. *Ind. Eng. Chem. Res.* **2001**, *40* (23), 5246–5254.  
doi:10.1021/ie001035a
39. Preller, A. C. N. *Numerical modelling of flow through packed beds of uniform spheres*: Potchefstroom, 2011.